



Published in final edited form as:

Tomography. 2017 June ; 3(2): 105–113. doi:10.18383/j.tom.2017.00006.

Language Mapping Using T2-Prepared BOLD Functional MRI in the Presence of Large Susceptibility Artifacts—Initial Results in Patients With Brain Tumor and Epilepsy

Jun Hua^{1,2}, Xinyuan Miao^{1,2}, Shruti Agarwal³, Chetan Bettegowda⁴, Alfredo Quiñones-Hinojosa⁵, John Lateralra⁶, Peter C. M. Van Zijl^{1,2}, James J. Pekar^{1,2}, and Jay J. Pillai³

¹F. M. Kirby Research Center for Functional Brain Imaging, Kennedy Krieger Institute, Baltimore, Maryland ²Neurosection, Division of MRI Research, Russell H. Morgan Department of Radiology and Radiological Science, Johns Hopkins University School of Medicine, Baltimore, Maryland ³Division of Neuroradiology, Russell H. Morgan Department of Radiology and Radiological Science, Johns Hopkins University School of Medicine, Baltimore, Maryland ⁴Neurosurgery, Johns Hopkins University School of Medicine, Baltimore, Maryland ⁵Neurological Surgery, Mayo Clinic, Jacksonville, Florida ⁶Department of Neurology, Johns Hopkins University School of Medicine, Baltimore, Maryland

Abstract

At present, presurgical functional mapping is the most prevalent clinical application of functional magnetic resonance imaging (fMRI). Signal dropouts and distortions caused by susceptibility effects in the current standard echo planar imaging (EPI)-based fMRI images are well-known problems and pose a major hurdle for the application of fMRI in several brain regions, many of which are related to language mapping in presurgical planning. Such artifacts are particularly problematic in patients with previous surgical resection cavities, craniotomy hardware, hemorrhage, and vascular malformation. A recently developed T2-prepared (T2prep) fMRI approach showed negligible distortion and dropouts in the entire brain even in the presence of large susceptibility effects. Here, we present initial results comparing T2prep- and multiband EPI-fMRI scans for presurgical language mapping using a sentence completion task in patients with brain tumor and epilepsy. In all patients scanned, T2prep-fMRI showed minimal image artifacts (distortion and dropout) and greater functional sensitivity than EPI-fMRI around the lesions containing blood products and in air-filled cavities. This enhanced sensitivity in T2prep-fMRI was also evidenced by the fact that functional activation during the sentence completion task was detected with T2prep-fMRI but not with EPI-fMRI in the affected areas with the same statistical threshold, whereas cerebrovascular reactivity during a breath-hold task was preserved in these same regions, implying intact neurovascular coupling in these patients. Although further investigations are required to validate these findings with invasive methods such as direct cortical

This is an open access article under the CC BY-NC-ND license (<http://creativecommons.org/licenses/by-nc-nd/4.0/>).

Corresponding Author: Jun Hua, PhD, Johns Hopkins University School of Medicine, Department of Radiology, Kennedy Krieger Institute, F. M. Kirby Research Center for Functional Brain Imaging, 707 N Broadway, Baltimore, MD, 21205; jhua@mri.jhu.edu.

Disclosures: No disclosures to report.

Conflict of Interest: None reported.

stimulation mapping as the gold standard, this approach provides an alternative method for performing fMRI in brain regions with large susceptibility effects.

Keywords

presurgical; implant; hemorrhage; dropout; distortion

INTRODUCTION

Presurgical functional mapping in patients with brain tumor and epilepsy is increasingly performed in large medical centers across the United States and worldwide (1–4). In patients with brain tumor, because of the infiltrative nature of most gliomas, complete surgical tumor removal is often impossible. To accomplish a maximal tumor resection for optimal therapeutic effect and simultaneously preserve neurological function and quality of life, a critical balance must be sought between the extent of resection and risk of postprocedural neurological deficit due to inadvertent injury to adjacent healthy functional (also known as “eloquent”) brain tissue. A similar concern exists with resection of other focal brain lesions such as vascular malformations and epileptogenic lesions such as malformations of cortical development. Thus, individual-based brain mapping of critical brain functions, such as sensorimotor and language, and accurate information on hemispheric dominance are of utmost importance for neurosurgeons to decide which surgical options are appropriate and whether less-invasive therapeutic approaches such as radiotherapy should be considered.

Blood oxygenation level-dependent (BOLD) functional magnetic resonance imaging (fMRI) has revolutionized the non-invasive assessment of human brain function. Shortly after its invention, it was used to locate sensorimotor and language areas in patients with brain tumor (5–7). Since then, substantial evidence has been established for the reliability of presurgical fMRI in patients with brain tumor and epilepsy (2, 6, 8–13). As a noninvasive technique, fMRI can provide critical information on brain function preoperatively, thus helping to reduce the need for invasive diagnostic procedures such as intraoperative cortical stimulation mapping.

Currently, gradient-echo (GRE) echo planar imaging (EPI) is the method of choice for most BOLD fMRI studies. However, the well-known geometric distortion and signal dropouts in EPI BOLD images caused by large magnetic susceptibility effects have hampered its application in some brain areas (14). In a normal brain, regions close to air cavities are usually the most affected by susceptibility artifacts, which typically include the orbitofrontal and temporal lobes. For instance, many brain studies using EPI BOLD fMRI at 3 Tesla (T) or lower fields have reported difficulties in detecting neuronal activation in regions such as inferior temporal (with a language task) (15, 16), medial temporal (memory task) (17), anterior temporal (face recognition) (18), and olfactory cortex (in both frontal and temporal lobes) (19). Many of these areas are particularly relevant for language localization, a primary diagnostic aim in presurgical mapping. Furthermore, such susceptibility artifacts become more severe in the presence of magnetic resonance (MR)-compatible metal head implants (20–23), such as metallic dental fillings and braces (24–26).

For presurgical fMRI, a significant subset of patients is affected by the distortion and dropout artifacts (thus, compromised sensitivity) in EPI BOLD, presenting a significant barrier for proper evaluation and interpretation of fMRI results, particularly in the following occasions:

1. Signal voids and distortions in regions close to surgical resection cavities and/or craniotomy hardware. This is a problem in almost *all* patients with prior resections who undergo presurgical fMRI in anticipation of additional surgery (27). About 25% of our presurgical mapping referrals at the Johns Hopkins Hospital fall into this category. These regions, understandably, are particularly important for presurgical planning and surgical outcome assessment; yet, the susceptibility artifacts impair the ability of EPI BOLD fMRI to map such eloquent cortex.
2. Artifacts in regions close to calcified structures, hemorrhages (eg, in vascular malformation) (28), and lesions that contain hemosiderin.
3. Artifacts due to intracranial metallic implants and devices placed during surgery or endovascular intervention, such as MR-compatible aneurysm clips or endovascular coils.

Recently, we demonstrated a whole-brain T2-prepared (T2prep) BOLD fMRI approach (29, 30) that uses a spin preparation module (T2prep) (31–33) before readout to induce T2-weighted BOLD effects for fMRI. This approach separates BOLD contrast generation from image acquisition, thereby opening the possibility to use readout sequences that are less sensitive to susceptibility artifacts (dropout and distortion) compared with EPI. We have shown in normal human brains that by adopting a 3-dimensional (3D) fast GRE (also known as turbo field echo, TFE, or TurboFLASH) readout with short echo time (TE), a sequence typically used in anatomical imaging, the T2prep BOLD fMRI approach showed minimal signal dropout and distortion across the entire brain even in the presence of metallic dental braces (34), allowing clear access to regions near air-filled cavities and metal objects that are often inaccessible with conventional EPI BOLD (14–26).

In the current study, we report initial results for using T2prep BOLD fMRI for presurgical language mapping in patients with brain tumor and epilepsy on 3 T clinical MRI scanners and evaluate the results by comparing with the current standard GRE EPI BOLD fMRI performed in the same patients.

METHODOLOGY

Four patients (female = 1; male = 3; age, 27–57 years; range, 39.5 ± 12.7 years; see Table 1 for more information) were recruited for this pilot study. Planned MRI scans were completed in all patients with satisfactory image quality. This study was approved by the Johns Hopkins Institutional Review Board, and written informed consent was obtained from each patient.

All scans were performed on a 3 T Philips MRI scanner (Philips Healthcare, Best, The Netherlands). A 32-channel phased-array head coil was used for radiofrequency reception

and a body coil for transmit. A respiratory belt was placed around the patient's chest during the MRI scans. The following scans were performed for each patient:

1. 3D T1-weighted magnetization-prepared rapid acquisition GRE (MPRAGE) scan (TR/inversion time/TE = 2300/ 900/3.5 milliseconds; voxel = 1 mm isotropic; 176 slices).
2. T2-weighted fluid attenuated inversion recovery (FLAIR) scan (TR/inversion time/TE = 9000/2500/116 milliseconds; voxel = $0.7 \times 0.7 \times 3$ mm³; 50 slices).
3. T2prep BOLD fMRI (TR = 2000 milliseconds; flip angle = 20°; T2prep effective TE = 50 milliseconds; voxel = $3.75 \times 3.75 \times 4$ mm³; 40 slices; no gap; parallel imaging or SENSE = 2×1.5 (AP \times FH), single-shot 3D turbo field echo readout, also known as 3D fast GRE, centric phase encoding profile starting from the center of k-space, TR_{GRE}/TE_{GRE} = 3.2/1.34 milliseconds).
4. 2-dimensional GRE EPI BOLD fMRI (TR = 2000 milliseconds; flip angle = 80°; TE = 30 milliseconds; voxel = $3.75 \times 3.75 \times 4$ mm³; multiband or blipped-CAIPI = 2; single-shot EPI readout; and fat suppression).

Typical imaging parameters for presurgical fMRI used clinically were chosen for T2prep and GRE EPI BOLD fMRI scans (matched between the 2 scans). Linear-only and linear plus optimized high-order shim (35) were applied in T2prep BOLD and EPI, respectively. Note that all EPI images were acquired with advanced parallel imaging technique (multiband or blipped-CAIPI) (36), and were shimmed with optimal high-order method and distortion-corrected (35). Therefore, these images represent the best-quality EPI images with least possible dropout and distortion on state-of-the-art clinical MRI scanners.

A sentence completion task typically used for language mapping clinically (37, 38) was adopted in this study. It consists of 3 blocks of 40-second control and 40-second active periods, followed by a 20-second control period in the end (total duration, 260 seconds). During the control period, strings of scrambled letters were presented on a screen and the patients were instructed to look at them. During the active period, the patients were asked to read (silently) a meaningful English sentence with 1 word missing presented every 5 seconds and to complete the sentence with at least 1 proper word. The sentence completion task is expected to activate mainly key language regions in the brain including the inferior frontal and superior temporal lobes. In addition to the sentence completion task, all patients were also instructed to perform a breath-hold task, consisting of 4 blocks of 40-second normal breathing, 4-second inhalation, and 16-second breath holding, followed by a 20-second normal breathing period in the end (total duration, 260 seconds). This task was routinely performed in our clinical scans to evaluate potential impairment of neurovascular coupling in these patients (3). All instructions in the sentence completion and breath-hold tasks were delivered using a projector from the back of the magnet onto a screen fixed on the head coil. Both paradigms were programmed using E-Prime 2.0 (Science Plus Group, The Netherlands). Each patient was asked to perform the sentence completion and breath-hold tasks twice during a T2prep BOLD and an EPI BOLD scan, respectively (ie, a total of 4 fMRI scans for each patient). The order of the fMRI scans was pseudorandomized among patients.

The statistical parametric mapping (SPM) software package (Version 12, Wellcome Trust Centre for Neuroimaging, London, UK; <http://www.fil.ion.ucl.ac.uk/spm/>) and other in-house code programmed in Matlab (MathWorks, Natick, MA) were used for image analysis. Functional MRI images were motion-corrected using the realignment routine in SPM. Slice timing correction was performed for 2D multi-slice EPI BOLD scans, but this was not needed for 3D T2prep BOLD scans. Anatomical images were coregistered with fMRI images. As presurgical fMRI is usually analyzed on an individual basis, the normalization step of fMRI images to the Montreal Neurological Institute (MNI) space was not performed. A general linear model was used to detect functional activation (adjusted $P < .05$; cluster size, 3). Motion parameters estimated from the realignment routine and time courses recorded from the respiratory belt were regressed out. The relative signal change ($\Delta S/S$) was calculated as the difference signal between control and active periods divided by average baseline signal. To avoid transition signals between the control and active periods, only data points acquired during the second half of the control and active periods were used to calculate the average signals. Temporal signal-to-noise ratio (tSNR) was taken as the signal divided by standard deviation along the time course in each voxel. Contrast-to-noise ratio (CNR) was defined as the product of tSNR and ($\Delta S/S$). Two-sample two-tailed t -tests with unequal variances were performed to compare the results from the 2 fMRI methods. Both activation-based and regions of interest (ROIs)-based analyses were conducted. In activation-based analysis, functional results in each method were averaged over all voxels that had met the criteria for activation detection in respective scans (suprathreshold voxels: same statistical threshold for both methods as described above, but the selection of voxels can be different in each method). In ROI-based analysis, a direct comparison between the 2 fMRI methods was allowed by using the same ROIs (thus same selection of voxels) in both fMRI methods. Two ROIs—the inferior frontal lobe and the superior temporal lobe—were manually delineated on the anatomical (FLAIR) images for each patient, which were then overlaid onto all fMRI scans from the same patient for signal averaging. Both ROIs include important language regions: the inferior frontal lobe includes the Broca's area (left) and its homologue (right); the superior temporal lobe include the Wernicke's area (left) and its homologue (right).

RESULTS

Figure 1 shows typical GRE EPI and T2prep BOLD and FLAIR images acquired in this study with original resolution in respective scans before preprocessing (therefore slices not perfectly aligned). Patient 2 (Table 1) had a hemorrhagic glioblastoma in the left frontal opercular and insular cortex, causing signal dropouts in EPI images due to the presence of blood products in the tumoral regions. Image distortion and dropout in the frontal cortex and in some basal regions of the brain were also apparent in EPI images, as commonly shown previously in normal brain scans (14–20). In contrast, the T2prep BOLD images showed minimal distortion and dropout across the entire brain, including the hemorrhagic tumor areas, and the shape of the images closely resembled that of the anatomical (FLAIR) images.

Figure 2 shows fMRI results from a patient (patient 1 in Table 1) with a glioblastoma in the left temporal lobe containing blood products in the cavity, causing severe dropouts in the EPI images (Figure 2C). The sentence completion task normally activates both the inferior

frontal and superior temporal lobes. Activation in the inferior frontal areas (yellow arrow) in both hemispheres were detected on both the T2prep and GRE EPI BOLD scans. However, activation in the superior temporal area (red arrow) was considerably diminished around the dropout regions in the EPI BOLD scan compared with the T2prep BOLD scan. No significant activation in the right temporal lobe was detected in this patient in both the T2prep and EPI BOLD scans. In the breath-hold task (Figures 2, E and F), positive cerebrovascular reactivity (CVR) was detected in most normal-appearing brain regions, including the areas surrounding the glioblastoma, using T2prep BOLD fMRI.

Similarly, Figure 3 shows fMRI results from a patient with epilepsy with a larger cavernous malformation in the left temporal lobe and a much smaller one in the anterior left frontal lobe (patient 4 in Table 1), causing signal dropouts in the areas in the EPI images (Figure 3C). Activation in the left inferior frontal lobe (yellow arrow) was detected in the T2prep BOLD scan (Figure 3, A and B) but not the GRE EPI BOLD scan (Figures 3, C and D). No significant activation in the superior temporal lobe (red arrow) was detected in this patient with both the T2prep and EPI BOLD scans. In the breath-hold task (Figure 3, E and F), positive CVR was detected in most normal-appearing brain regions in both hemispheres including the areas surrounding the lesion using T2prep BOLD fMRI.

Table 2 summarizes the individual quantitative fMRI results for language mapping using the sentence completion task from all patients. The relative signal change ($\Delta S/S$), tSNR, and CNR were comparable between T2prep and EPI BOLD scans in all patients in activation-based analysis (described in Methodology). In all 4 patients studied, lesions were adjacent to the inferior frontal and/or superior temporal areas, which resulted in substantial susceptibility artifacts (signal dropout) in the EPI images. In the ROI-based analyses, although tSNR values were still comparable between the 2 methods in these regions, relative signal change ($\Delta S/S$) and CNR were both lower in EPI BOLD scans compared with T2prep BOLD scans in all patients. Because of the location of the lesions, the inferior frontal area was more affected in patients 2–4, whereas the superior temporal area was more affected in patient 1. Note that in the ROI-based analyses, some voxels included may not have passed the activation detection threshold described in Methodology. Therefore, the averaged signal changes over all voxels in the ROI were smaller than those from all activated voxels in respective scans in all patients. None of the ($\Delta S/S$) results with a negative mean value was significantly different from zero.

Table 3 compares the quantitative fMRI results between the T2prep and GRE EPI BOLD approaches from the sentence completion and breath-hold tasks (4 patients, 2 scans/tasks per patient using each method; therefore, $n = 8$). Consistent with individual results shown in Table 2, the relative signal change ($\Delta S/S$), tSNR, and CNR were all comparable between the 2 methods in the respective activated voxels. In the inferior frontal and superior temporal lobes, tSNR values were comparable between the 2 methods, whereas $\Delta S/S$ and CNR were both significantly lower in EPI BOLD scans than in T2prep BOLD scans.

DISCUSSION

Presurgical functional mapping is currently the most prevalent clinical application of fMRI and is the only one with approved AMA (American Medical Association) billing CPT (Current Procedural Terminology) codes (<http://www.asfnr.org/cpt-codes/>). Susceptibility artifacts, including image distortion and signal dropouts, in EPI-based BOLD fMRI images have been a major confound for the analysis and clinical interpretation of fMRI results in several important brain regions (14–26), many of which are particularly related to language mapping in presurgical planning. In addition, such artifacts affect a significant subset of patients undergoing presurgical fMRI, such as patients with previous surgical resection cavities, craniotomy hardware, calcified structures, hemorrhage, vascular malformation, and lesions that contain hemosiderin in the brain (27, 28). A number of methods have been developed to ameliorate this problem, including spin echo-based sequences, gradient spin echo, spiral MRI, advanced shimming techniques, z-shim, various methods for near metal imaging, and many others (30). Recently, we have developed an alternative approach for BOLD fMRI that can achieve whole-brain fMRI images with typical temporal and spatial resolution for fMRI, and image quality (in terms of distortion and dropouts) that is comparable with standard anatomical MR images (such as MPRAGE and FLAIR), even in the presence of large susceptibility effects such as in areas near air cavities and metal objects in the brain (29, 30, 34).

We further evaluated the utility of the T2prep BOLD fMRI approach for presurgical planning in patients who suffer from substantial susceptibility artifacts in EPI images. We present herein our initial results for comparing T2prep BOLD and GRE EPI BOLD fMRI scans for presurgical language mapping in patients with brain tumor and epilepsy. Susceptibility-induced signal dropouts and distortion around lesions containing blood products and air-filled cavities were apparent in EPI BOLD images, whereas such artifacts were minimal in T2prep BOLD images in the same regions (Figures 1–3). In all patients studied, these artifacts affected important language regions such as the inferior frontal and superior temporal areas. Functional activation during the sentence completion task was detected with T2prep BOLD fMRI but not with EPI BOLD fMRI in the affected areas with the same statistical threshold (Figures 2 and 3). We attribute this mainly to a substantially impaired functional sensitivity in EPI BOLD due to large susceptibility effects in these regions. This was supported by subsequent quantitative analysis of the fMRI results both at the individual (Table 2) and group (Table 3) levels. As expected, functional results (S/S , tSNR, and CNR) were comparable between the 2 methods in voxels that met respective activation detection criteria in each scan, as only voxels with sufficient functional sensitivity in each method were included in signal averaging. However, significant decreases in S/S and CNR in the inferior frontal and superior temporal areas were found in EPI BOLD compared with T2prep BOLD. Note that tSNR was still comparable between the 2 methods in these regions. This can be explained by the fact that as physiological noise is dominant in fMRI, a decrease in tSNR may not be proportional to the MR signal loss (39–42). This also indicates that even when complete signal dropout is avoided and reasonable tSNR is achieved, the underlying BOLD sensitivity (CNR) can be much diminished in regions affected by large susceptibility artifacts, as discussed by others (43–45).

Hypercapnia induced by a functional task such as breath-hold is often used to probe the integrity of neurovascular coupling in the brain of patients undergoing presurgical fMRI (3). This is particularly important for the interpretation of presurgical fMRI results in patients. In all patients scanned, positive CVR during the breath-hold task was detected in most normal-appearing brain regions using T2prep BOLD fMRI, which includes the areas showing substantial signal losses in EPI BOLD images. This provides further evidence for our hypothesis that the lack of activation in some language regions affected by susceptibility artifacts in EPI BOLD scans (for instance, Figures 2 and 3) was mainly due to reduced functional sensitivity compared to T2prep BOLD fMRI, rather than impaired neurovascular coupling in these patients.

One trade-off in T2prep BOLD fMRI is that it gives T2-weighted spin echo BOLD contrast, which is less sensitive to the BOLD effect than the T2*-weighted GRE BOLD contrast. Although this is a disadvantage in regions not affected by susceptibility artifacts, the sensitivity (CNR) in T2prep BOLD was significantly higher than that of GRE-EPI in brain regions with large susceptibility effects. Whereas, the CNR in small susceptibility areas was relatively higher in EPI BOLD, the T2prep BOLD data still provided sufficient detection power for neuronal activities in these regions (30). However, in regions with large susceptibility effects, GRE EPI often failed to detect meaningful signal changes, whereas T2prep BOLD showed preserved CNR across the entire brain. Whether such a trade-off in sensitivity between regions with small and large susceptibility artifacts is worthwhile for presurgical fMRI in all brain regions (sensorimotor, language, and memory) requires further investigation. Our initial results showed here suggest that T2prep BOLD may be a promising alternative method for presurgical fMRI when large susceptibility artifacts are present in EPI BOLD images. As presurgical fMRI protocols often consist of several anatomical and functional scans, this can be feasibly incorporated into existing clinical workflow. The operator can determine whether the T2prep BOLD sequence should be run based on evaluation of initial scout images, a GRE EPI scan without functional task (typically for a few seconds), field maps, or other anatomical images for assessment of susceptibility artifacts.

The sentence completion task used in this study is commonly used for presurgical language mapping in clinics, which is expected to invoke neuronal activation in both the inferior frontal and superior temporal areas in both hemispheres of a normal brain (37, 38). In some patients (Figures 2 and 3), significant activation during the sentence completion task was detected only in the inferior frontal but not in the superior temporal areas, or only in one of the hemispheres with both the T2prep and EPI BOLD scans, while neurovascular coupling seemed to be intact as indicated by the fMRI results during the breath-hold scans. This could be because of certain pathological reasons (37, 38, 46, 47), but further validation is warranted using direct cortical stimulation, the “gold standard” method.

In summary, we showed that T2prep BOLD fMRI has potential for presurgical language mapping in patients with brain tumor and epilepsy. These initial data on a small group of patients show higher functional sensitivity in brain regions affected by large susceptibility artifacts than in the current standard EPI BOLD fMRI scans. To make T2prep BOLD a clinically useful technique, validation in a larger cohort and with invasive methods such as

direct cortical stimulation as the gold standard is required. If successful, we expect this approach to benefit a significant subset of patients undergoing presurgical fMRI by providing an alternative method for performing fMRI in brain regions with large susceptibility effects.

Acknowledgments

The authors thank Mr. Joseph S. Gillen, Mrs. Terri Lee Brawner, Ms. Kathleen A. Kahl, and Ms. Ivana Kusevic for experimental assistance. This project was supported by the National Institute of Biomedical Imaging and Bioengineering of the National Institutes of Health through R21 grant R21EB023538 and resource grant P41 EB015909. Equipment used in the study was manufactured by Philips. Dr. van Zijl is a paid lecturer for Philips Healthcare. This arrangement has been approved by Johns Hopkins University in accordance with its conflict of interest policies.

Abbreviations

fMRI	Functional magnetic resonance imaging
EPI	echo planar imaging
T2prep	T2-prepared
BOLD	blood oxygenation level-dependent
GRE	gradient-echo
MR	magnetic resonance
FLAIR	fluid attenuated inversion recovery
3D	3-dimensional
TE	echo time
TR	repetition time
tSNR	temporal signal-to-noise ratio
CNR	contrast-to-noise ratio
ROIs	regions of interest
CVR	cerebrovascular reactivity

References

1. Stippich C, Rapps N, Dreyhaupt J, Durst A, Kress B, Nennig E, Tronnier VM, Sartor K. Localizing and lateralizing language in patients with brain tumors: feasibility of routine preoperative functional MR imaging in 81 consecutive patients. *Radiology*. 2007; 243(3):828–836. [PubMed: 17517936]
2. Binder JR, Swanson SJ, Hammeke TA, Morris GL, Mueller WM, Fischer M, Benbadis S, Frost JA, Rao SM, Houghton VM. Determination of language dominance using functional MRI: a comparison with the Wada test. *Neurology*. 1996; 46(4):978–984. [PubMed: 8780076]
3. Zaca D, Hua J, Pillai JJ. Cerebrovascular reactivity mapping for brain tumor pre-surgical planning. *World J Clin Oncol*. 2011; 2(7):289–298. [PubMed: 21773079]
4. Pillai JJ. Clinical applications of functional MRI. *Neuroimaging Clin N Am*. 2014; 24(4)

5. Jack CR Jr, Thompson RM, Butts RK, Sharbrough FW, Kelly PJ, Hanson DP, Riederer SJ, Ehman RL, Hangiandreou NJ, Cascino GD. Sensory motor cortex: correlation of presurgical mapping with functional MR imaging and invasive cortical mapping. *Radiology*. 1994; 190(1):85–92. [PubMed: 8259434]
6. FitzGerald DB, Cosgrove GR, Ronner S, Jiang H, Buchbinder BR, Belliveau JW, Rosen BR, Benson RR. Location of language in the cortex: a comparison between functional MR imaging and electrocortical stimulation. *AJNR Am J Neuroradiol*. 1997; 18(8):1529–1539. [PubMed: 9296196]
7. Desmond JE, Sum JM, Wagner AD, Demb JB, Shear PK, Glover GH, Gabrieli JD, Morrell MJ. Functional MRI measurement of language lateralization in Wada-tested patients. *Brain*. 1995; 118(Pt 6):1411–1419. [PubMed: 8595473]
8. Yetkin FZ, Mueller WM, Morris GL, McAuliffe TL, Ulmer JL, Cox RW, Daniels DL, Haughton VM. Functional MR activation correlated with intraoperative cortical mapping. *AJNR Am J Neuroradiol*. 1997; 18(7):1311–1315. [PubMed: 9282861]
9. Rutten GJ, van Rijen PC, van Veelen CW, Ramsey NF. Language area localization with three-dimensional functional magnetic resonance imaging matches intra-sulcal electrostimulation in Broca's area. *Ann Neurol*. 1999; 46(3):405–408. [PubMed: 10482272]
10. Rutten GJ, Ramsey NF, van Rijen PC, Noordmans HJ, van Veelen CW. Development of a functional magnetic resonance imaging protocol for intraoperative localization of critical temporoparietal language areas. *Ann Neurol*. 2002; 51(3):350–360. [PubMed: 11891830]
11. Benson RR, FitzGerald DB, LeSueur LL, Kennedy DN, Kwong KK, Buchbinder BR, Davis TL, Weisskoff RM, Talavage TM, Logan WJ, Cosgrove GR, Belliveau JW, Rosen BR. Language dominance determined by whole brain functional MRI in patients with brain lesions. *Neurology*. 1999; 52(4):798–809. [PubMed: 10078731]
12. Sabbah P, Chassoux F, Leveque C, Landre E, Baudoin-Chial S, Devaux B, Mann M, Godon-Hardy S, Nioche C, Ait-Ameur A, Sarrazin JL, Chodkiewicz JP, Cordo-liani YS. Functional MR imaging in assessment of language dominance in epileptic patients. *Neuroimage*. 2003; 18(2):460–467. [PubMed: 12595199]
13. Bizzi A, Blasi V, Falini A, Ferroli P, Cadioli M, Danesi U, Aquino D, Marras C, Caldiroli D, Broggi G. Presurgical functional MR imaging of language and motor functions: validation with intraoperative electrocortical mapping. *Radiology*. 2008; 248(2):579–589. [PubMed: 18539893]
14. Horwitz B, Simonyan KP. PET neuroimaging. plenty of studies still need to be performed: comment on Cumming: "PET neuroimaging: the white elephant packs his trunk?". *Neuroimage*. 2014; 84:1101–1103. [PubMed: 23954490]
15. Devlin JT, Russell RP, Davis MH, Price CJ, Wilson J, Moss HE, Matthews PM, Tyler LK. Susceptibility-induced loss of signal: comparing PET and fMRI on a semantic task. *Neuroimage*. 2000; 11(6 Pt 1):589–600. [PubMed: 10860788]
16. Halai AD, Welbourne SR, Embleton K, Parkes LM. A comparison of dual gradient-echo and spin-echo fMRI of the inferior temporal lobe. *Hum Brain Mapp*. 2014; 35(8):4118–4128. [PubMed: 24677506]
17. Schacter DL, Wagner AD. Medial temporal lobe activations in fMRI and PET studies of episodic encoding and retrieval. *Hippocampus*. 1999; 9(1):7–24. [PubMed: 10088896]
18. Axelrod V, Yovel G. The challenge of localizing the anterior temporal face area: a possible solution. *Neuroimage*. 2013; 81:371–380. [PubMed: 23684864]
19. Yang QX, Dardzinski BJ, Li S, Eslinger PJ, Smith MB. Multi-gradient echo with susceptibility inhomogeneity compensation (MGESIC): demonstration of fMRI in the olfactory cortex at 3.0 T. *Magn Reson Med*. 1997; 37(3):331–335. [PubMed: 9055220]
20. Ludeke KM, Roschmann P, Tischler R. Susceptibility artefacts in NMR imaging. *Magn Reson Imaging*. 1985; 3(4):329–343. [PubMed: 4088009]
21. New PF, Rosen BR, Brady TJ, Buonanno FS, Kistler JP, Burt CT, Hinshaw WS, Newhouse JH, Pohost GM, Taveras JM. Potential hazards and artifacts of ferromagnetic and nonferromagnetic surgical and dental materials and devices in nuclear magnetic resonance imaging. *Radiology*. 1983; 147(1):139–148. [PubMed: 6828719]

22. Laakman RW, Kaufman B, Han JS, Nelson AD, Clampitt M, O'Block AM, Haaga JR, Alford RJ. MR imaging in patients with metallic implants. *Radiology*. 1985; 157(3):711–714. [PubMed: 4059558]
23. Hinshaw DB Jr, Holshouser BA, Engstrom HI, Tjan AH, Christiansen EL, Catelli WF. Dental material artifacts on MR images. *Radiology*. 1988; 166(3):777–779. [PubMed: 3340777]
24. Zho SY, Kim MO, Lee KW, Kim DH. Artifact reduction from metallic dental materials in T1-weighted spin-echo imaging at 3.0 tesla. *J Magn Reson Imaging*. 2013; 37(2):471–478. [PubMed: 22941956]
25. Schenck JF. The role of magnetic susceptibility in magnetic resonance imaging: MRI magnetic compatibility of the first and second kinds. *Med Phys*. 1996; 23(6):815–850. [PubMed: 8798169]
26. Shellock, FG. Reference Manual for Magnetic Resonance Safety, Implants, and Devices. Playa Del Rey, CA: Biomedical Research Publishing Group; 2014.
27. Geissler A, Matt E, Fischmeister F, Wurnig M, Dymerska B, Knosp E, Feucht M, Trattinig S, Auff E, Fitch WT, Robinson S, Beisteiner R. Differential functional benefits of ultra highfield MR systems within the language network. *Neuroimage*. 2014; 103:163–170. [PubMed: 25255049]
28. Stippich, C. Clinical Functional MRI: Presurgical Functional Neuroimaging. 2. New York: Springer; 2015.
29. Hua, J., Jones, CK., Qin, Q., van Zijl, PCM. T2-prepared blood-oxygenation-level-dependent (BOLD) fMRI using single-shot 3D fast gradient echo (GRE) sequence with whole brain coverage at 7T; Paper presented at: Proceedings of 21st Annual Meeting ISMRM; Salt Lake City, USA. 2013.
30. Hua J, Qin Q, van Zijl PC, Pekar JJ, Jones CK. Whole-brain three-dimensional T2-weighted BOLD functional magnetic resonance imaging at 7 Tesla. *Magn Reson Med*. 2014; 72(6):1530–1540. [PubMed: 24338901]
31. Parrish T, Hu X. A new T2 preparation technique for ultrafast gradient-echo sequence. *Magn Reson Med*. 1994; 32(5):652–657. [PubMed: 7808267]
32. Wright KB, Klocke FJ, Deshpande VS, Zheng J, Harris KR, Tang R, Finn JP, Li D. Assessment of regional differences in myocardial blood flow using T2-weighted 3D BOLD imaging. *Magn Reson Med*. 2001; 46(3):573–578. [PubMed: 11550251]
33. Denolin V, Metens T. Three-dimensional BOLD fMRI with spin-echo characteristics using T2 magnetization preparation and echo-planar readouts. *Magn Reson Med*. 2003; 50(1):132–144. [PubMed: 12815688]
34. Wu, Y., Woods, D., Stern, MT., Blair, NIS., Airan, RD., Pekar, JJ., van Zijl, PCM., Hua, J. Whole brain BOLD functional MRI in the presence of metallic orthodontic braces; Paper presented at: Proceedings of 23rd Annual Meeting ISMRM; Toronto, Canada. 2015.
35. Schar M, Kozerke S, Fischer SE, Boesiger P. Cardiac SSFP imaging at 3 Tesla. *Magn Reson Med*. 2004; 51(4):799–806. [PubMed: 15065254]
36. Setsompop K, Gagoski BA, Polimeni JR, Witzel T, Wedeen VJ, Wald LL. Blipped-controlled aliasing in parallel imaging for simultaneous multislice echo planar imaging with reduced g-factor penalty. *Magn Reson Med*. 2012; 67(5):1210–1224. [PubMed: 21858868]
37. Zaca D, Nickerson JP, Deib G, Pillai JJ. Effectiveness of four different clinical fMRI paradigms for preoperative regional determination of language lateralization in patients with brain tumors. *Neuroradiology*. 2012; 54(9):1015–1025. [PubMed: 22744798]
38. Zaca D, Jarso S, Pillai JJ. Role of semantic paradigms for optimization of language mapping in clinical FMRI studies. *AJNR Am J Neuroradiol*. 2013; 34(10):1966–1971. [PubMed: 23788599]
39. Gonzalez-Castillo J, Roopchansingh V, Bandettini PA, Bodurka J. Physiological noise effects on the flip angle selection in BOLD fMRI. *Neuroimage*. 2011; 54(4):2764–2778. [PubMed: 21073963]
40. Kruger G, Kastrup A, Glover GH. Neuroimaging at 1.5 T and 3.0 T: comparison of oxygenation-sensitive magnetic resonance imaging. *Magn Reson Med*. 2001; 45(4):595–604. [PubMed: 11283987]
41. Kruger G, Glover GH. Physiological noise in oxygenation-sensitive magnetic resonance imaging. *Magn Reson Med*. 2001; 46(4):631–637. [PubMed: 11590638]

42. Triantafyllou C, Hoge RD, Krueger G, Wiggins CJ, Potthast A, Wiggins GC, Wald LL. Comparison of physiological noise at 1.5 T, 3 T and 7 T and optimization of fMRI acquisition parameters. *Neuroimage*. 2005; 26(1):243–250. [PubMed: 15862224]
43. Hutton C, Bork A, Josephs O, Deichmann R, Ashburner J, Turner R. Image distortion correction in fMRI: A quantitative evaluation. *Neuroimage*. 2002; 16(1):217–240. [PubMed: 11969330]
44. Deichmann R, Josephs O, Hutton C, Corfield DR, Turner R. Compensation of susceptibility-induced BOLD sensitivity losses in echo-planar fMRI imaging. *Neuroim-age*. 2002; 15(1):120–135.
45. Deichmann R, Gottfried JA, Hutton C, Turner R. Optimized EPI for fMRI studies of the orbitofrontal cortex. *Neuroimage*. 2003; 19(2 Pt 1):430–441. [PubMed: 12814592]
46. Pillai JJ, Williams HT, Faro S. Functional imaging in temporal lobe epilepsy. *Semin Ultrasound CT MR*. 2007; 28(6):437–450. [PubMed: 18075000]
47. Zaca D, Agarwal S, Gujar SK, Sair HI, Pillai JJ. Special considerations/technical limitations of blood-oxygen-level-dependent functional magnetic resonance imaging. *Neuroimaging Clin N Am*. 2014; 24(4):705–715. [PubMed: 25441509]

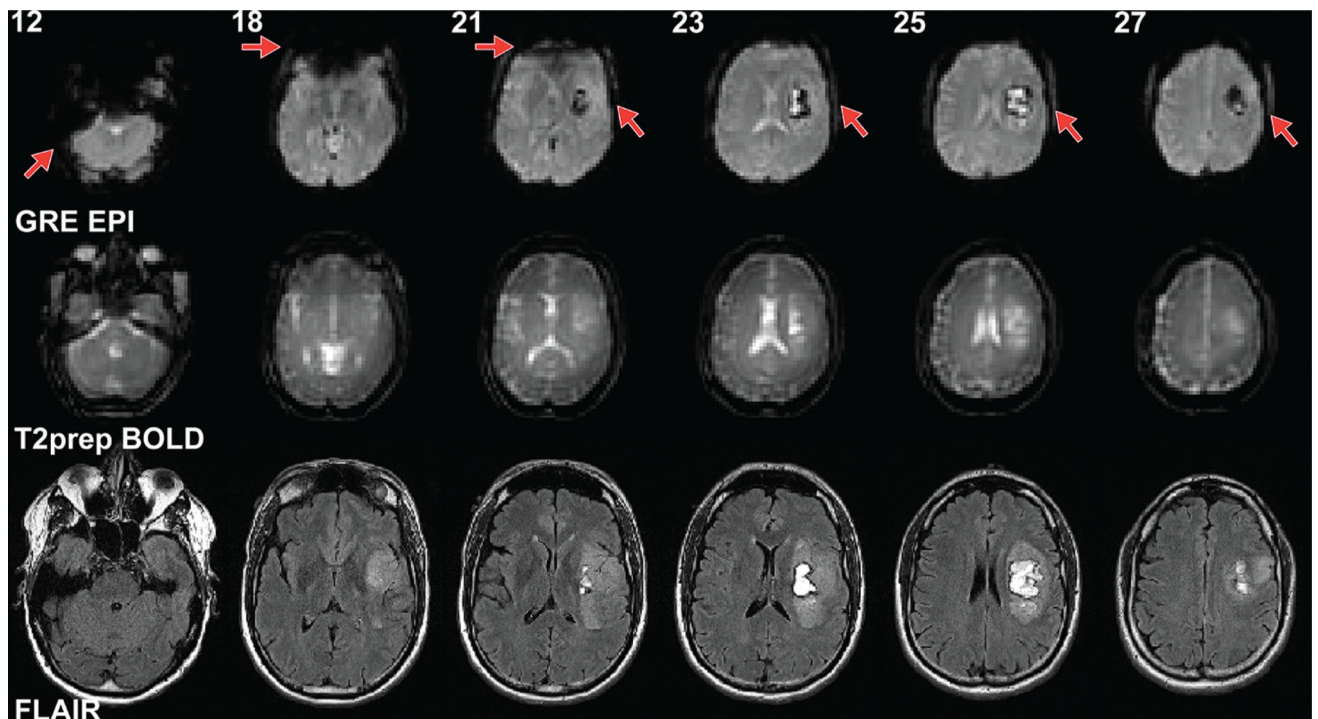


Figure 1. Representative echo planar imaging (EPI) and T2-prepared (T2prep) blood oxygenation level-dependent (BOLD) functional magnetic resonance imaging (fMRI), and anatomical (fluid attenuated inversion recovery [FLAIR]) images from patient 2 described in Table 1. Raw images at original spatial resolution in respective scans before preprocessing are shown. Slice numbers in the EPI and T2prep BOLD scans are indicated at the top of each column. Slices from different scans are approximately aligned. Note that anatomical (FLAIR) images were acquired at a much higher spatial resolution than the EPI and BOLD fMRI images. Linear shim was applied in T2prep BOLD. Optimal high-order shim was used in gradient-echo (GRE) EPI BOLD.

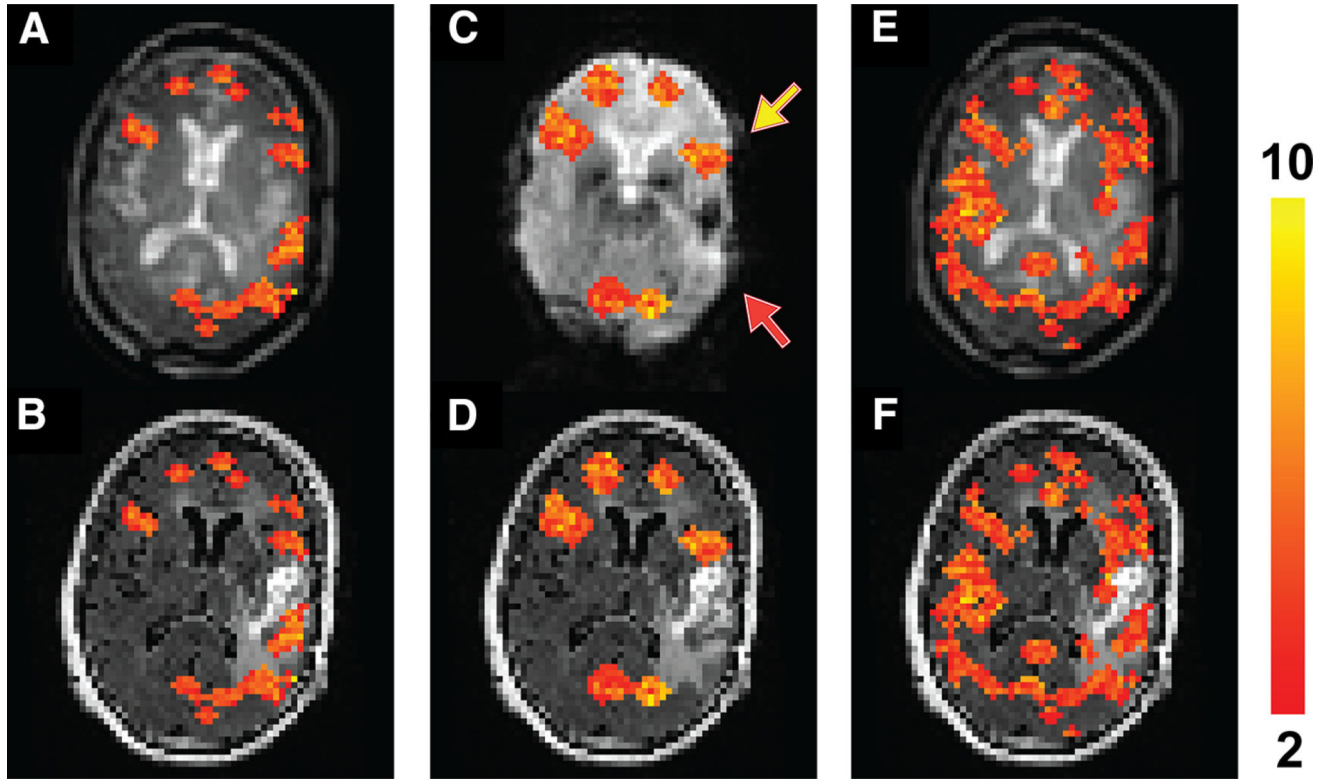


Figure 2.

Functional MRI results from *patient 1* described in Table 1. Activated voxels during the *sentence completion* task using *T2prep BOLD* fMRI overlaid on the original T2prep BOLD and coregistered anatomical (FLAIR) images, respectively (A, B). Activated voxels during the *sentence completion* task using *GRE EPI BOLD* fMRI overlaid on the EPI and anatomical (FLAIR) images, respectively (C, D). Voxels with positive cerebrovascular reactivity (CVR) (“activated”) during the breath-hold task using *T2prep BOLD* fMRI overlaid on the T2prep BOLD and anatomical (FLAIR) images, respectively (E, F). Note that the anatomical (FLAIR) images displayed here were down-sampled to match the original spatial resolution of the fMRI images. The activated voxels are highlighted with their *t*-scores. The scale bar on the right indicates the range of *t*-scores in the highlighted voxels. The yellow and red arrows point to the inferior frontal and superior temporal lobes, respectively (2 important language regions in the brain).

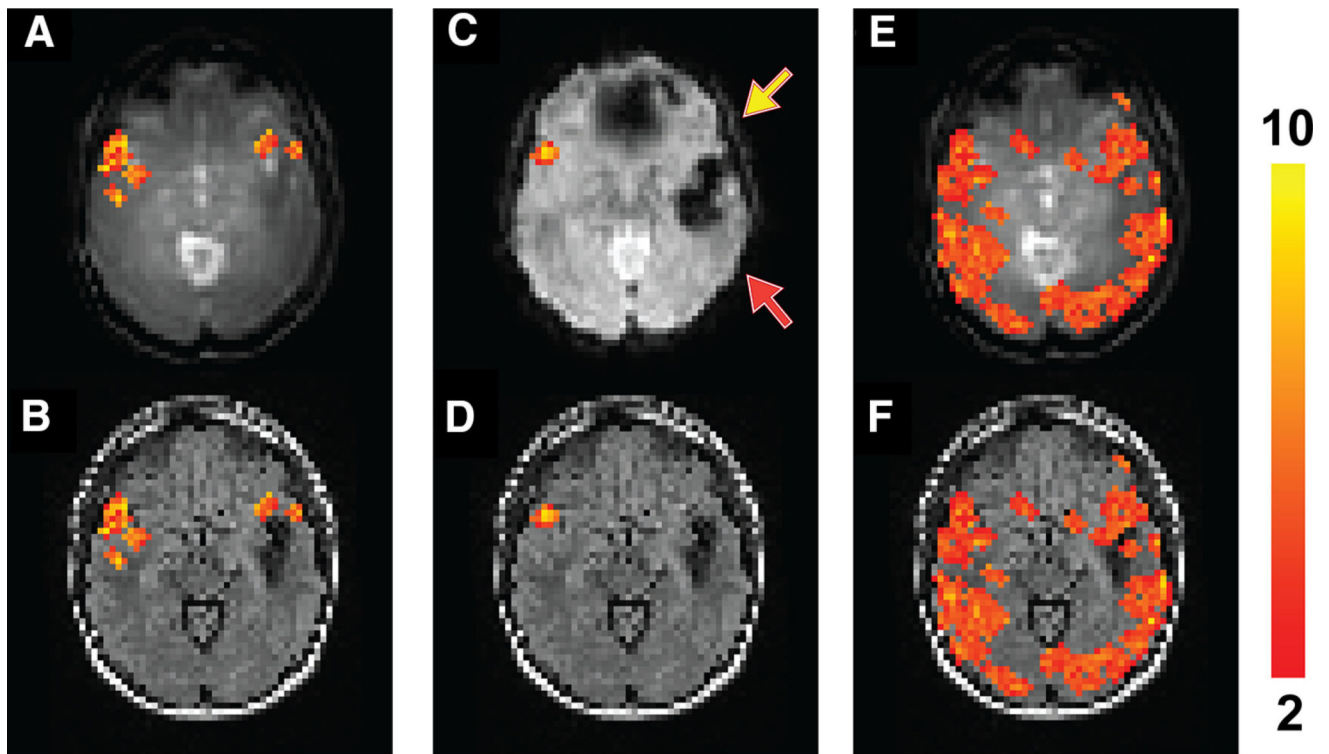


Figure 3. Functional MRI results from *patient 4* described in Table 1. Activated voxels during the *sentence completion* task using *T2prep BOLD* fMRI overlaid on the original T2prep BOLD and coregistered anatomical (FLAIR) images, respectively (A, B). Activated voxels during the *sentence completion* task using *GRE EPI BOLD* fMRI overlaid on the EPI and anatomical (FLAIR) images, respectively (C, D). Voxels with positive CVR (“activated”) during the breath-hold task using *T2prep BOLD* fMRI overlaid on the T2prep BOLD and anatomical (FLAIR) images, respectively (E, F). Note that the anatomical (FLAIR) images displayed here were down-sampled to match the original spatial resolution of the fMRI images. The activated voxels are highlighted with their t -scores. The scale bar on the right indicates the range of t -scores in the highlighted voxels. The yellow and red arrows point to the inferior frontal and superior temporal lobes, respectively (two important language regions in the brain).

Table 1

Demographic Data and Clinical Information for Patients

Pt. No.	Sex	Age (years)	Type	Lesion Location	Description
1	M	57	Tumor	Left temporal	A patient with residual left temporal lobe glioblastoma (WHO Grade IV). The very high FLAIR regions represent blood products in the cavity, whereas the lower (but still abnormal) signal intensity in more extensive regions represents a combination of vasogenic edema and nonenhancing tumor infiltration.
2	M	39	Tumor	Left frontal opercular and insular	A patient with hemorrhagic glioblastoma.
3	F	35	Epilepsy	Left anterior temporal	A patient with left temporal lobe resection cavity and craniotomy hardware from prior surgery.
4	M	27	Epilepsy	Left anterior frontal and left superior temporal	The two lesions seen in the patient are cavernous malformations.

Abbreviations: Pt., Patient; FLAIR, fluid attenuated inversion recovery.

Individual Quantitative fMRI Results for Language Mapping (Sentence Completion) from all Patients

Table 2

	Patient 1	Patient 2	Patient 3	Patient 4	Average
<i>Activated voxels in respective scans^a</i>					
<i>T2prep</i>					
S/S (%) ^c	0.54 ± 0.29	0.87 ± 0.13	1.14 ± 0.25	0.64 ± 0.40	0.80 ± 0.23
iSNR ^c	57.54 ± 24.63	76.99 ± 24.56	46.77 ± 19.90	30.99 ± 16.23	53.07 ± 16.73
CNR ^c	31.11 ± 7.09	67.13 ± 3.09	53.32 ± 4.96	19.87 ± 6.53	42.86 ± 18.47
<i>EPI</i>					
S/S (%)	0.67 ± 0.12	0.79 ± 0.14	1.06 ± 0.21	0.57 ± 0.18	0.77 ± 0.18
iSNR	50.64 ± 26.67	76.30 ± 34.15	46.12 ± 22.27	31.04 ± 19.20	51.03 ± 16.30
CNR	34.15 ± 3.20	59.99 ± 4.78	48.89 ± 4.60	17.69 ± 3.54	40.18 ± 15.90
<i>Inferior frontal lobe including the Broca's area^b</i>					
<i>T2prep</i>					
S/S (%)	0.20 ± 0.05	0.14 ± 0.03	0.94 ± 0.21	0.25 ± 0.09	0.38 ± 0.32
iSNR	41.87 ± 22.19	46.02 ± 26.32	41.78 ± 10.76	36.95 ± 11.36	41.65 ± 3.21
CNR	8.41 ± 1.11	6.51 ± 0.79	39.27 ± 2.21	9.24 ± 1.02	15.86 ± 13.55
<i>EPI</i>					
S/S (%)	0.05 ± 0.07	-0.16 ± 0.10	-0.28 ± 0.29	-0.01 ± 0.22	-0.10 ± 0.13
iSNR	40.23 ± 41.05	36.83 ± 31.80	40.36 ± 32.80	42.34 ± 24.66	39.94 ± 1.98
CNR	2.01 ± 2.80	-5.89 ± 3.14	-11.30 ± 9.58	-0.42 ± 5.42	-3.90 ± 5.14
<i>Superior temporal lobe including the Wernicke's area^b</i>					
<i>T2prep</i>					
S/S (%)	0.17 ± 0.05	0.16 ± 0.05	0.37 ± 0.11	0.17 ± 0.11	0.22 ± 0.09
iSNR	77.92 ± 31.90	91.17 ± 33.70	53.70 ± 28.58	39.99 ± 25.30	65.70 ± 20.02
CNR	13.25 ± 1.61	14.59 ± 1.81	19.87 ± 3.24	6.87 ± 2.78	13.64 ± 4.63
<i>EPI</i>					
S/S (%)	-0.06 ± 0.04	0.02 ± 0.05	0.21 ± 0.15	0.03 ± 0.09	0.05 ± 0.10
iSNR	70.16 ± 57.22	96.70 ± 56.06	54.20 ± 31.01	55.42 ± 28.27	69.12 ± 17.12

	Patient 1	Patient 2	Patient 3	Patient 4	Average
CNR	-4.21 ±2.42	1.93 ±2.92	11.38 ±4.65	1.56 ± 2.62	2.67 ± 5.59

Abbreviations: T2prep, T2-prepared; tSNR, temporal signal-to-noise ratio; CNR, contrast-to-noise ratio; EPI, echo planar imaging.

^a Signals averaged over all activated voxels in respective scans.

^b Signals averaged over all voxels (including voxels that did not meet the activation detection criteria described in Methodology) in the inferior frontal and superior temporal lobes, respectively. Regions of interest (ROIs) were manually drawn on the anatomical (FLAIR) image for each subject. The same ROI was used for all scans from each patient.

^c Relative signal change (S/S), tSNR, and CNR are defined in Methodology.

Table 3Statistical Comparison of Quantitative fMRI Results Between T2prep and EPI BOLD fMRI (n = 8)[†]

	T2prep	EPI	P
<i>Activated voxels in respective scans^a</i>			
S/S (%) ^c	1.58 ± 0.43	1.62 ± 0.46	.872
tSNR ^c	61.33 ± 13.20	58.11 ± 14.07	.877
CNR ^c	97.51 ± 24.77	94.52 ± 20.55	.823
<i>Inferior frontal lobe including the Broca's area^b</i>			
S/S (%)	0.73 ± 0.37	0.23 ± 0.11	.001 [*]
tSNR	44.66 ± 5.11	38.99 ± 6.12	.576
CNR	33.45 ± 17.15	5.96 ± 4.39	.012 [*]
<i>Superior temporal lobe including the Wernicke's area^b</i>			
S/S (%)	0.47 ± 0.25	0.25 ± 0.14	.049 [*]
tSNR	68.89 ± 20.17	64.12 ± 18.03	.828
CNR	31.79 ± 8.02	14.20 ± 4.81	.042 [*]

Abbreviations: T2prep, T2-prepared; tSNR, temporal signal-to-noise ratio; CNR, contrast-to-noise ratio; EPI, echo planar imaging.

[†] Each method was performed twice (2 tasks: sentence completion and breath-hold) in all 4 patients, therefore n = 8.

^{*} P values < .05.

^a Signals averaged over all activated voxels in respective scans.

^b Signals averaged over all voxels (including voxels that did not meet the activation detection criteria described in Methodology) in the inferior frontal and superior temporal lobes, respectively. Regions of interest (ROIs) were manually drawn on the anatomical (FLAIR) image for each patient. The same ROI was used for all scans from each subject.

^c Relative signal change (S/S), tSNR, and CNR are defined in Methodology.